

Comparison of imaging flow cytometry and microscopy for freshwater algal bloom detection

Sabina R. Gifford, Ann St. Amand, Jennifer L. Graham, Guy M. Foster, Cory Sauve, Denise Clark & Hannah Schroeder-Larkins

To cite this article: Sabina R. Gifford, Ann St. Amand, Jennifer L. Graham, Guy M. Foster, Cory Sauve, Denise Clark & Hannah Schroeder-Larkins (2024) Comparison of imaging flow cytometry and microscopy for freshwater algal bloom detection, Lake and Reservoir Management, 40:3, 221-235, DOI: [10.1080/10402381.2024.2370828](https://doi.org/10.1080/10402381.2024.2370828)

To link to this article: <https://doi.org/10.1080/10402381.2024.2370828>



This work was authored as part of the Contributor's official duties as an Employee of the United States Government and is therefore a work of the United States Government. In accordance with 17 U.S.C. 105, no copyright protection is available for such works under U.S. Law.



[View supplementary material](#)



Published online: 09 Aug 2024.



[Submit your article to this journal](#)



Article views: 430



[View related articles](#)



[View Crossmark data](#)

Comparison of imaging flow cytometry and microscopy for freshwater algal bloom detection

Sabina R. Gifford^a, Ann St. Amand^b, Jennifer L. Graham^a, Guy M. Foster^a, Cory Sauve^b, Denise Clark^b and Hannah Schroeder-Larkins^b

^aU.S. Geological Survey, Troy, NY, USA; ^bPhycoTech, Inc, St. Joseph, MI, USA

ABSTRACT

Gifford SR, St. Amand A, Graham JL, Foster GM, Sauve C, Clark D, Schroeder-Larkins H. 2024. Comparison of imaging flow cytometry and microscopy for freshwater algal bloom detection. *Lake Reserv Manage.* 40:221–235.

Imaging flow cytometry (IFC) is an emerging tool that allows for rapid identification and enumeration of phytoplankton in freshwater systems. However, few studies have assessed the effects of preservation on IFC results or compared live IFC and microscopy results in freshwater systems. Understanding the effects of preservation and differences between IFC and microscopy will improve interpretation of these data and inform strategies to use IFC-based approaches in freshwater systems. Our study objectives were to compare IFC and phase contrast with epifluorescence microscopy as techniques for phytoplankton identification and enumeration, and the effects of sample preservation with an emphasis on taxa forming harmful cyanobacterial blooms (HCBs). During June through October 2020, samples were collected from 2 lakes in the Finger Lakes region of New York. Live and preserved samples were analyzed by laboratory-based IFC, and preserved samples were analyzed by microscopy. The IFC approach captured community dynamics while detecting potential cyanobacterial bloom-forming taxa earlier and at lower abundances than microscopy. Laboratory-based IFC allowed for an intermediate level of taxonomic information when compared to microscopy, gross techniques, such as extracted chlorophyll *a* or fluorescence sensors, and field-based operation of IFC approaches. The laboratory-based application of IFC in this study allowed receipt of results in 5 d or less, a substantial improvement over microscopy, which can be time-consuming to conduct. However, the laboratory-based IFC approach had some limitations. Imaging flow cytometry-estimated biovolume may be less accurate than microscopy for some taxa because of the algorithms used to calculate biovolume, particularly for chrysophytes and coccoid cyanobacteria. Colonial dissociation during preservation appeared to affect detection of *Microcystis* by IFC less than for other fragile bloom-forming taxa like chrysophytes. Our study results advance understanding of how IFC may translate to field-based approaches for early harmful algal bloom indicators in freshwater.

KEYWORDS


Cyanobacteria; freshwater HABs; imaging flow cytometry; methods validation; preservation effects

Harmful algal blooms (HABs) are increasingly a global concern in waterbodies used for drinking-water supply and recreation because of the potential risks posed to human and ecosystem health (Paerl and Huisman 2009, Ndlela et al. 2016, Pick 2016, Chorus and Welker 2021). Monitoring phytoplankton communities is an important tool that has been widely used by water resource managers to track the presence and abundance of potential cyanotoxin-producing cyanobacteria, taste- and odor-producing phytoplankton, and other algae. Numerous sampling

strategies and analytical methods are used to assess phytoplankton biomass and community structure in freshwaters (Berkman and Canova 2007, Interstate Technology and Regulatory Council 2020, Chorus and Welker 2021).

Methods such as extracted chlorophyll *a* and chlorophyll fluorescence sensors estimate overall phytoplankton biomass (Foster et al. 2022). Other methods, like multichannel fluorescence sensors, estimate relative phytoplankton community composition but do not identify potential taxa of concern (Johnston et al. 2022). These methods are generally

CONTACT Sabina R. Gifford  srjifford@usgs.gov

 Supplemental data for this article can be accessed online at <https://doi.org/10.1080/10402381.2024.2370828>.

This work was authored as part of the Contributor's official duties as an Employee of the United States Government and is therefore a work of the United States Government. In accordance with 17 U.S.C. 105, no copyright protection is available for such works under U.S. Law. This is an Open Access article that has been identified as being free of known restrictions under copyright law, including all related and neighboring rights <https://creativecommons.org/publicdomain/mark/1.0/>. You can copy, modify, distribute and perform the work, even for commercial purposes, all without asking permission. The terms on which this article has been published allow the posting of the Accepted Manuscript in a repository by the author(s) or with their consent.

inexpensive and are not time intensive but lack the taxonomic resolution that is often needed when characterizing HABs. Phytoplankton identification and enumeration by microscopy has traditionally been the gold standard for HAB monitoring (Interstate Technology and Regulatory Council 2020). The taxonomic resolution afforded by this approach is essential to understanding algal bloom dynamics, spatiotemporal variability, diversity, and biogeography. From a resource management perspective, knowing the composition of an algal bloom can help inform management decisions to protect human health (Graham et al. 2008).

Traditional microscopy provides quantitative genus or species level data but is costly and requires a high level of taxonomic expertise (Chorus and Welker 2021). The level of information provided also depends on the quality of the microscope and the expertise of the taxonomist. Microscopy methods range in sophistication from basic counts of natural units (i.e., colonies, filaments, or single cells) to get an idea of overall community composition to more quantitative measures of abundance and biovolume. There are many quantitative approaches, including Sedgewick–Rafter chambers, the Utermöhl method, and 2-hydroxypropyl methacrylate (HPMA) fixed mounts that allow fluorescence microscopy and archival use for later reference (Crumpton, 1987, American Public Health Association 2022). Preparation, enumeration, and identification using these methodologies require a substantial time investment. For example, the time it takes to enumerate phytoplankton using the Utermöhl method may range between 2 and 10 h, depending on the sample (Edler and Elbrächter 2010).

A relatively new, rapidly advancing method for phytoplankton analysis is imaging flow cytometry (IFC). Available technologies for automating phytoplankton identification and enumeration using IFC are reviewed in Dashkova et al. (2017). Imaging flow cytometry can be used to assess phytoplankton assemblages by passing water through an instrument in flow. Particles flow past a laser beam, which triggers the instrument to capture an image. Image analysis techniques then produce a suite of additional measurements that can be used in a classification model and to calculate biovolume. Processing time is reduced

compared to traditional microscopy while maintaining an intermediate level of taxonomic detail (Dashkova et al. 2017). The increased capacity and reduced processing time make IFC a potentially effective method for HAB monitoring and large-scale ecological assessment. In addition, IFC may be used in laboratory- and field-based applications. The image classification algorithms that IFC uses to classify phytoplankton are instrument specific, and the training image libraries can be augmented or enhanced to cater to a specific environment or application (Sosik and Olson 2007, Dashkova et al. 2017).

Most IFC applications have focused on marine systems (Dashkova et al. 2017, Spanbauer et al. 2020), where the approach has been successfully used as a near-real-time field-based indicator of potentially harmful taxa like *Karenia brevis* and other dinoflagellates that can cause red tides (Campbell et al. 2010, 2013, Harred and Campbell 2014). The phytoplankton that cause HABs in marine environments have morphology and bloom habits different from those in freshwater (e.g., cyanobacteria), and it is uncertain how IFC techniques developed for marine systems will perform in freshwater. Studies of use of cytometry to estimate marine filamentous cyanobacteria blooms show promise, but rigorous comparisons with microscopy have not been conducted in freshwater systems (Kraft et al. 2021).

Preservation of samples is often necessary for microscopy methods because of delays between sample collection and sample analysis; however, inaccuracies may be introduced by any method that requires preservation (Vaughan et al. 2022). Studies have shown a positive bias in cyanobacteria cell counts in preserved samples compared to live samples measured with IFC (Graham et al. 2018). The formation of aggregates has been noted as a source of error in samples preserved with Lugol's iodine because IFC has difficulty differentiating individual taxa within an aggregate (Zarauz and Irigoien 2008). We have observed that the formation of aggregates may be more pronounced in samples preserved with Lugol's compared to samples preserved with glutaraldehyde.

The goals of this study were to assess (1) how freshwater HAB-forming taxa identification and enumeration in split samples compare as analyzed

by microscopy and IFC methods, and (2) how preservation affects the efficacy of IFC analysis. This effort will inform our understanding of the advantages and disadvantages of HAB-forming taxa identification and enumeration by IFC when compared to microscopy. Laboratory-based use of IFC could provide substantial reductions in cost and in result delivery time for monitoring programs focused on public health protection. The study results are a first step in understanding how IFC use may translate to field-based approaches for early HAB indicators in freshwater. In addition, to the best of our knowledge, this is the first study to compare live and glutaraldehyde-preserved samples enumerated using IFC methods.

Methods

Study sites and sample collection

Phytoplankton samples from Seneca and Owasco lakes, in the Finger Lakes region of New York, were collected every 2 weeks from June through October 2020. These lakes, used for recreation and municipal water supply, experience cyanobacteria HABs of predominantly *Microcystis* spp., and microcystins are often detected in surface accumulations (New York State Department of Environmental Conservation et al. 2019). Seneca and Owasco lakes are large, meso-oligotrophic lakes that are low in turbidity (2020 seasonal means: 0.3 FNU and 1.0 FNU, respectively; both $n=10$) and dissolved organic carbon (DOC, 2020 seasonal means: 2.68 mg/L and 2.34 mg/L, respectively; both $n=10$) (U.S. Geological Survey 2016). Low nonalgal particle and DOC concentrations in our samples limited the extraneous factors that may interfere with IFC analysis, allowing us to focus on the effects of preservation and the comparison of methods for phytoplankton identification and enumeration.

In total, 20 samples were collected, 10 from each lake. Samples were collected at 1 m depth using a vertical 8 L VanDorn sampler from open water locations at the north end of each lake (Seneca: USGS Station 425027076564401; Owasco: USGS Station 425327076313601). Samples were immediately homogenized and split using a Teflon churn. Two subsamples were collected from the churn for phytoplankton analysis: a live, unpreserved sample and a sample preserved with

glutaraldehyde (by adding 25% glutaraldehyde to a final concentration of 0.25%). Glutaraldehyde was used to preserve the fluorescence properties of the phytoplankton and reduce morphological distortion compared to other preservatives (American Public Health Association 2022).

For the duration of the study, a Xylem Yellow Springs Instruments EXO2 (Yellow Springs, OH) multiparameter sonde collected continuous water-quality data, including chlorophyll fluorescence, at the same location and depth at which discrete samples were collected in each lake. Continuous water quality data were collected every 15 min in accordance with USGS protocols (U.S. Geological Survey variously dated; Wagner et al. 2006) and are available through the USGS National Water Information System (U.S. Geological Survey 2016).

Sample analysis

Live samples were analyzed by IFC, and preserved samples were split for analyses by IFC and microscopy. All analyses were conducted by PhycoTech, Inc. (St. Joseph, MI). Identification and enumeration using microscopy were conducted on a BX 51 Olympus microscope with Phase Nomarski and fluorescence capability, using HPMa mounted slides, a minimum of 15 random fields to a count threshold of at least 400 natural units, and a size range of detection from 0.9 μm to 25 mm (American Public Health Association 2022, PhycoTech Inc). Smaller cyanobacteria taxa were counted and identified using fluorescence-enabled microscopy. Magnification used ranged from 100 \times to 1000 \times ; magnifications used to identify individual taxa are available in Perkins et al. (2021). Biovolume was calculated based on measuring cell and colonial dimensions on up to 10 natural units per taxon within each sample. Taxon-specific calculations were combinations of simple geometric figures applied to cells and adjusted based on estimates of cells per natural unit (Olrik et al. 1998, Hillebrand et al. 1999). Imaging flow cytometry was conducted using a laboratory-based Imaging Flow CytoBot (IFCB, McLane Research Laboratories, Inc., East Falmouth, MA). The IFCB was calibrated to best detect particles $\sim 50 \mu\text{m}$ in size with a detection range from 5 to 150 μm (McLane Research

Laboratories Inc 2020). The IFCB most reliably counts suspended particles between 5 and 150 μm , but the imaging mechanism is triggered by particles as small as 2 μm (Olson and Sosik 2007). Samples were not concentrated or diluted prior to analysis. Sample volumes (1.0–4.7 mL) and run times (4–20 min) varied based on phytoplankton density to ensure that at a minimum 500 images were collected per sample. Between 642 and 3063 high-resolution images (~ 3.4 pixels per 1 μm) were produced per sample run, considerably more than were analyzed by microscopy. Sample volume, run time, and number of images collected for each sample are available in Gifford et al. (2023).

All images collected from the samples that were run through the IFCB were manually classified to the class or genus level by a trained taxonomist and later verified by an expert phycologist. Taxa below the 5 μm detection threshold that could not be reliably identified were placed in a “Miscellaneous” category. Similarly, all imperfect images that could not be identified, such as small flagellates entrained in detritus, partial images, and images with multiple taxa, were placed in an “Unclassified” category. Algal concentration and biovolume were calculated based on methods described in Olson and Sosik (2007) and a Matlab (MathWorks Matlab R2018b, Toolboxes- Curve Fitting, Deep Learning, Image Processing, Parallel Computing, Statistics and Machine Learning, DIPUM) script adapted from <https://github.com/hsosik/ifcb-analysis> (Release 1.0, September 13, 2016).

Data analysis

Both identification and enumeration methods included natural units, cell abundance, and biovolume. Our analysis focuses on cell abundance with a limited discussion of biovolume. We chose to focus on cell abundance because this is currently what is used in many HAB alert frameworks to protect public health (Chorus and Welker 2021, Ortiz et al. 2023). Data analysis focused on comparing the ability of the different methods to detect and quantify potentially harmful cyanotoxin-producing cyanobacteria (HCB) because of the potential human health risk

associated with these taxa. Taxonomic resolution was to the lowest identifiable level for each method, typically class or genus for the IFC and species for microscopy. Data were grouped into 9 different ecological functional groups for analysis: non-cyanotoxin-producing cyanobacteria (BG), cryptophytes/dinoflagellates (CP), chrysophytes/haptophytes/diatoms (DY), euglenophytes (E), chlorophytes (G), potential cyanotoxin-producing cyanobacteria (HCB), miscellaneous (M), unknown (U), and cyanobacteria taste and odor producers (TO). All IFC data are available in Gifford et al. (2023) and all microscopy data are available in Perkins et al. (2021).

The IFC methods cannot reliably count taxa $< 5 \mu\text{m}$; however, smaller taxa may still be detected (Olson and Sosik 2007) and were classified in the “Miscellaneous” category. The microscopic method used in this study is able to identify and enumerate taxa as small as 0.9 μm . In addition to using total cell abundances measured using microscopy (“Microscopy”) to make comparisons, we also used cell abundances of taxa with an average greatest axial linear dimension (GALD) greater than 5 μm (“Microscopy $> 5 \mu\text{m}$ ”) to match the published detection threshold of the IFCB.

Due to the relatively small sample size and paired nature of the data, exact sign tests were used to test for statistical differences in HCB abundance and biovolume among the 3 different methods (preserved microscopy, preserved IFC, and live IFC). Orthogonal regressions were drawn between live and preserved IFC estimates for total sample cell abundance and biovolume; this regression type was chosen to allow for the possibility of error in both measurements (Helsel et al. 2020). A summary analysis of single cells versus cells present in colonies was conducted for *Microcystis* spp. and *Uroglena* spp. during 2 identified bloom events. Data analyses and statistics were conducted in R version 4.2.1 using the *pracma* package for the orthogonal regressions and base R for the other statistical analyses (Borchers 2022, R Core Team 2022). Cellular abundance estimates (cells/mL) for the preserved IFC and preserved microscopy $> 5 \mu\text{m}$ methods were aggregated to the functional group level for each sample, square-root transformed, and used to calculate Bray–Curtis similarities between the

2 methods using PRIMER v7 software (Clarke and Gorley 2015).

Results

Comparison of algal identification and enumeration by imaging flow cytometry and microscopy

Based on microscopy, taxa smaller than $5\mu\text{m}$ dominated the phytoplankton community, comprising 33.5–96.4% (mean: 77.0%) and 26.7–99.7% (mean: 85.6%) of overall abundance in Owasco and Seneca lakes, respectively. When taxa smaller than $5\mu\text{m}$ were removed from microscopy cell counts, differences in abundance between the 2 methods were still present but less pronounced (Fig. 1). Overall, total cellular abundance estimates based on microscopy methods were higher

than IFC abundance estimates for both lakes (Fig. 1). As expected, this difference is largely due to the inclusion of taxa $<5\mu\text{m}$ in microscopy estimates; microscopy abundance estimates were significantly higher than both live and preserved IFC estimates (exact sign test, P value < 0.001 , $n=20$ for both comparisons). Differences between the 2 methods were not statistically significant when only taxa $>5\mu\text{m}$ were included in the microscopy abundance estimates (exact sign test, P value = 0.058, $n=20$ for both comparisons). Total phytoplankton abundances in live samples based on IFC were relatively low, ranging from 323 to 21,416 cells/mL (mean 4993 cells/mL) and 769 to 6803 cells/mL (mean 3198 cells/mL) in samples from Owasco and Seneca lakes, respectively. Total phytoplankton abundances in preserved samples based on IFC were similarly low

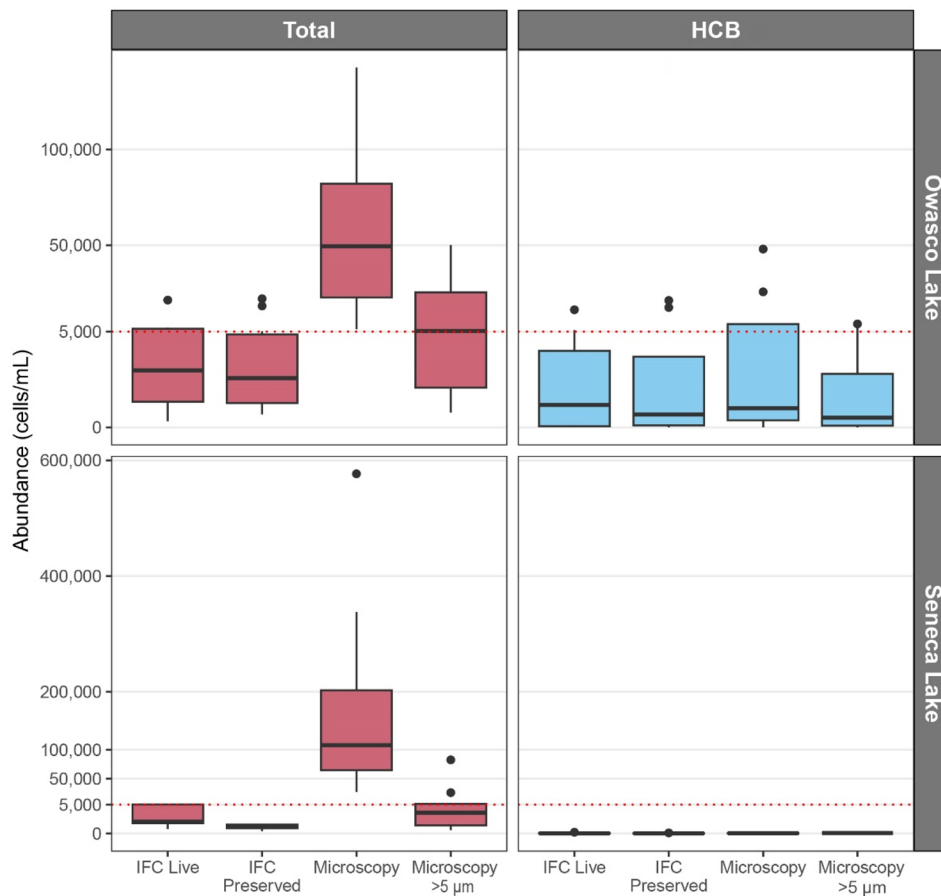


Figure 1. Total phytoplankton and potential cyanotoxin-producing cyanobacteria (HCB) abundance in samples collected from Owasco and Seneca lakes during Jun through Oct 2020. Live and preserved samples were measured using imaging flow cytometry (IFC) and preserved samples were measured using microscopy. The scale below the red dotted line is a factor of 10 lower than the rest of the graph to allow for visualization of low abundances. Box plots indicate the 25th, median, and 75th percentiles, with the whiskers extending to the largest (or smallest for the lower whisker) value no further than 1.5 times the interquartile range.

(Owasco: mean 5914 cells/mL, range 684–22,113 cells/mL; Seneca: mean 1197 cells/mL, range 398–1701 cells/mL). Cell abundance estimates based on microscopy were, on average, an order of magnitude higher in Owasco Lake (range 6247–136,207 cells/mL; mean 61,091 cells/mL), and almost 2 orders of magnitude higher in Seneca Lake (range 26,953–576,744 cells/mL; mean 170,631 cells/mL) than IFC abundance estimates (Supplemental Table S2).

Differences in cell abundance estimates between methods are smaller for HCB taxa abundance than for total phytoplankton abundance (Fig. 1). HCB abundance estimates based on microscopy averaged 1.9 times higher than the live IFC abundance estimates (range 0.3–4.5 times higher) and 1.2 times higher than the preserved IFC abundance estimates (range 0.2–3.0 times higher) but differences were not statistically significant (exact sign test, P value = 0.25, $n=9$ and P value = 0.62, $n=10$, respectively). All paired HCB cell abundance estimates were within one order of magnitude across all method comparisons.

Seasonal patterns in functional group abundance estimates based on IFC largely capture the dynamic and diverse community composition

patterns observed in the analyses by microscopy, especially in Owasco Lake (Fig. 2). Microscopy abundance estimates in both lakes were dominated by the BG functional group (i.e., cyanobacteria that are not known cyanotoxin producers; Fig. 2). Many of the cyanobacteria in the BG functional group were unicellular (<2 μ m) or small 4–8 celled colonial taxa at or just above the 5 μ m threshold used to exclude small taxa from this analysis.

In Owasco Lake, seasonal patterns in HCB abundance were similar between methods despite differences in overall abundance. The predominance of HCB increased throughout summer, peaked in late August, and declined through September (Fig. 2). BG taxa were more abundant later in the season (September and October), with higher abundances observed in samples analyzed by microscopy, where taxa <5 μ m in the Chroococcaceae family dominated (Supplemental Table S1). Although seasonal patterns in HCB and BG abundance were similar, there was a substantial amount of variability in overall community composition at the functional group level between the 2 methods (Bray–Curtis similarity: mean 54%, range 37–75%, $n=10$). Samples from the HCB bloom in August were some of the

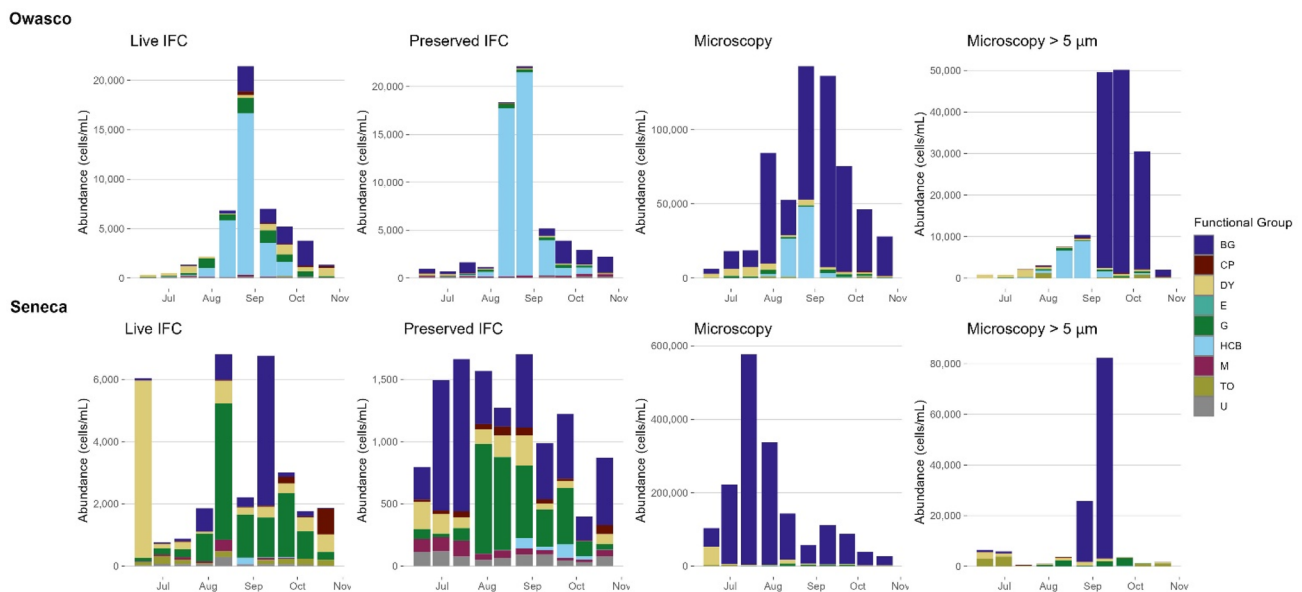


Figure 2. Phytoplankton community abundance and composition in samples collected from Owasco and Seneca lakes during Jun through Oct 2020. Live and preserved samples were measured using imaging flow cytometry (IFC) and preserved samples were measured using microscopy. Note that scale varies across graphs to allow visualization of low abundance groups. Community composition is defined by functional groups: BG, non-toxin-producing cyanobacteria; CP, cryptophytes/dinoflagellates; DY, chrysophytes/haptophytes/diatoms; E, euglenophytes; G, chlorophytes (green algae); HCB, potential cyanotoxin-producing cyanobacteria; M, miscellaneous; TO, potential taste- and odor-producing taxa; U, unknown.

samples with the highest similarities (Bray–Curtis similarity >70%) between methods.

In Seneca Lake, patterns in functional groups other than BG were largely obscured by the overwhelming dominance of taxa <5µm based on microscopy (Supplemental Table S1). When BG taxa were excluded, a chrysophyte bloom in June (specifically, *Uroglena* spp., a potential taste- and odor-producing taxa) became evident. The *Uroglena* spp. bloom was observed in the live IFC abundance (and biovolume) estimates, but not the preserved IFC estimates (Fig. 2, Supplemental Fig. S1). In contrast to Owasco Lake, HCB abundance remained low throughout the entire season and the phytoplankton community was dominated (>50% of cell abundance) in turn by chrysophytes, chlorophytes, and BG taxa (Fig. 2). Overall community composition at the functional group level was also more variable between the 2 methods in Seneca Lake (Bray–Curtis similarity: mean 41%, range 23–58%, $n=10$) than observed for Owasco Lake.

Harmful cyanobacteria bloom taxa were detected more often, and earlier in the season, by IFC than by microscopy. *Microcystis* spp. were the dominant HCB taxa (>98% of total HCB abundance) throughout the season in both lakes, despite differences in overall abundance. *Microcystis aeruginosa* was most common (>90% of total HCB abundance) and *Dolichospermum lemmermannii* was present in many samples. Based on IFC results, 85% (17/20) and 60% (12/20) of preserved and live samples, respectively, had detections of HCB taxa. By comparison, 50% (10/20) of samples analyzed by microscopy had HCB taxa detected. There were 10 samples

where HCB taxa were detected by both microscopy and preserved IFC methods (paired detections) and 9 samples with paired detections between the microscopy and live IFC methods. Mismatches were most often the result of low-level detections by the IFC of *Microcystis* spp. that were not detected by microscopy (Table 1). In both lakes, *Microcystis* spp. were detected by the IFC nearly a month before detection by microscopy (Table 1). In Owasco Lake, *Microcystis* spp. were consistently detected by live and preserved IFC samples, whereas in Seneca Lake, *Microcystis* spp. were generally detected earlier and at lower levels in the preserved samples than in the live samples (Table 1).

In contrast to abundance estimates, differences in seasonal patterns in functional group biovolumes among methods were largely driven by differences in the HCB group (Supplemental Fig. S1). Biovolume estimates of HCB taxa (overwhelmingly *Microcystis* spp. in the study systems) were significantly higher in the live IFC estimates than preserved IFC estimates (exact sign test, P value < 0.01, $n=12$) and were significantly higher than microscopy (exact sign test, P value = 0.02, $n=9$ and P value < 0.01, $n=10$, respectively).

Paired estimates of HCB biovolume were more variable than paired estimates of cell abundance among the 3 methods. However, variability was lower between the 2 preserved methods than between the 2 IFC methods. Preserved biovolume estimates by IFC were 10.8 times higher on average than estimates by microscopy (range 1.3–25.4 times higher; Supplemental Fig. S2). By comparison, biovolume estimates based on live IFC samples were 14.4 times higher on average than

Table 1. *Microcystis* spp. abundance in samples collected from Owasco and Seneca lakes during Jun through Oct 2020.

	<i>Microcystis</i> spp. abundance (cells/mL)									
	6/15	7/1	7/15	7/28	8/12	8/25	9/10	9/22	10/7	10/22
Owasco										
IFC _{live}	ND	24	59	739	5684	16,312	3307	1462	ND	10
IFC _{pres.}	ND	3	78	386	17,569	21,108	3685	845	676	23
Microscopy _{pres.}	ND	ND	ND	1269	25,702	48,019	3268	554	447	ND
Microscopy	ND	ND	ND	504	6695	8983	1482	44	310	ND
>5 µm _{pres.}										
Seneca	6/16	6/31	7/14	7/29	8/11	8/26	9/9	9/23	10/6	10/20
IFC _{live}	ND	ND	ND	ND	ND	141	ND	ND	ND	1
IFC _{pres.}	ND	ND	<1	1	5	21	25	95	27	1
Microscopy _{pres.}	ND	ND	ND	ND	ND	ND	28	25	ND	ND
Microscopy	ND	ND	ND	ND	ND	ND	ND	25	ND	ND
>5 µm _{pres.}										

Live and preserved samples were measured using imaging flow cytometry (IFC) and preserved samples were measured using microscopy. ND indicates that *Microcystis* spp. were not detected.

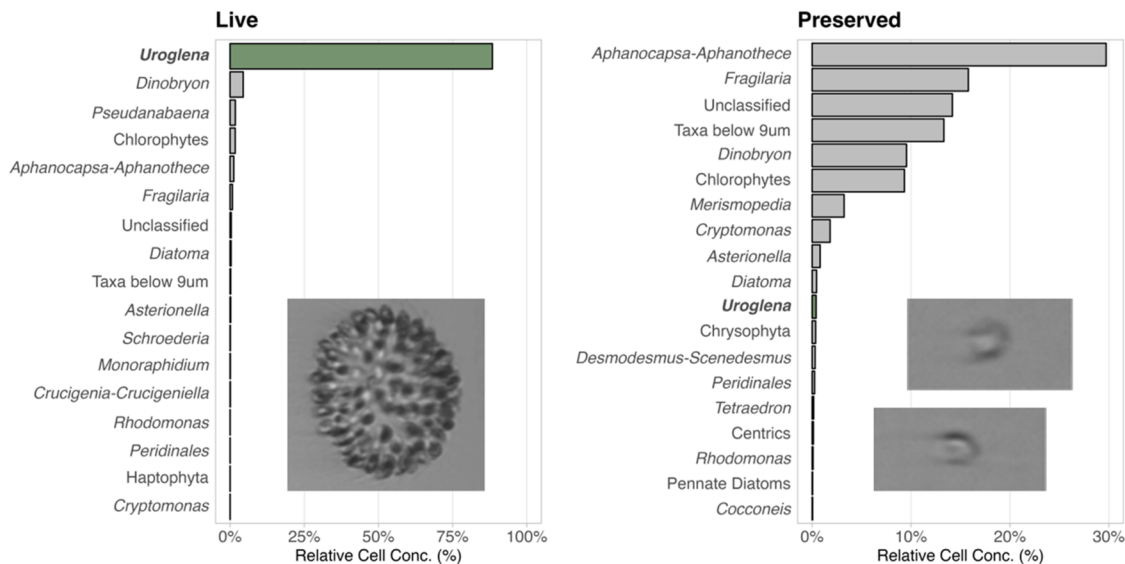


Figure 3. Relative cell concentration of taxa in live and glutaraldehyde preserved samples measured by imaging flow cytometry (IFC) in a sample collected from Seneca Lake on Jun 16, 2020. Characteristic images taken by IFC of *Uroglena* spp. in each sample type are shown.

preserved samples (range 0.3–133.4 times higher) and 39.5 times higher than the microscopy estimates (range 0.5–166.7 times higher). As might be expected due to their small size, taxa $<5\mu\text{m}$ contributed more to cell abundance (26.7–99.9% of total) than to biovolume (3.9–82.0% of total) for both lakes (Figs. 1 and 2; Supplemental Figs. S1 and S2; Supplemental Tables S2 and S3).

Preservation effects on analysis by imaging flow cytometry

Sample preservation is known to affect cell and colony morphology. Fragile colonial taxa, particularly chrysophytes, often fall apart when contained or preserved. Consequently, these taxa are often underdetected because of the small size of single cells or misidentified because of distortion (American Public Health Association 2022). The effects of colonial dissociation after preservation were illustrated in this dataset through blooms caused by 2 different taxa: *Uroglena* spp. and *M. aeruginosa*.

Uroglena spp. bloom

Based on results by live IFC, the chrysophyte *Uroglena* spp. dominated (about 90% of total abundance, 5,342 cells/mL) the Seneca Lake

phytoplankton community in mid June 2020; however, in results based on preserved IFC, *Uroglena* spp. represented $<1\%$ of total phytoplankton abundance (3 cells/mL; Fig. 3). In the live sample, *Uroglena* spp. were present as whole colonies (Fig. 3) whereas the *Uroglena* spp. in the preserved sample were present as single cells, close to the size detection threshold of the IFC. We have observed that *Uroglena* spp. cells distort upon preservation, making the morphology variable and difficult to identify. Dissociated single cells of *Uroglena* spp. with an average GALD $<5\mu\text{m}$ were the predominant form observed using microscopy (47,199 cells/mL). Therefore, many single-celled *Uroglena* were not represented in the “Microscopy $>5\mu\text{m}$ ” community (Fig. 2).

The June *Uroglena* spp. bloom was detected by multiple methods in Seneca Lake. In situ chlorophyll fluorescence sensors indicated a rapid increase and a seasonal maximum that was an order of magnitude higher than other peaks observed throughout the season. Similarly, laboratory-extracted chlorophyll *a* was 3 times higher than other observed values (Fig. 4). While both methods indicated a bloom was occurring, neither could be used to identify the causative division or taxa. Based on the live IFC and microscopy biovolume analyses, seasonal maxima

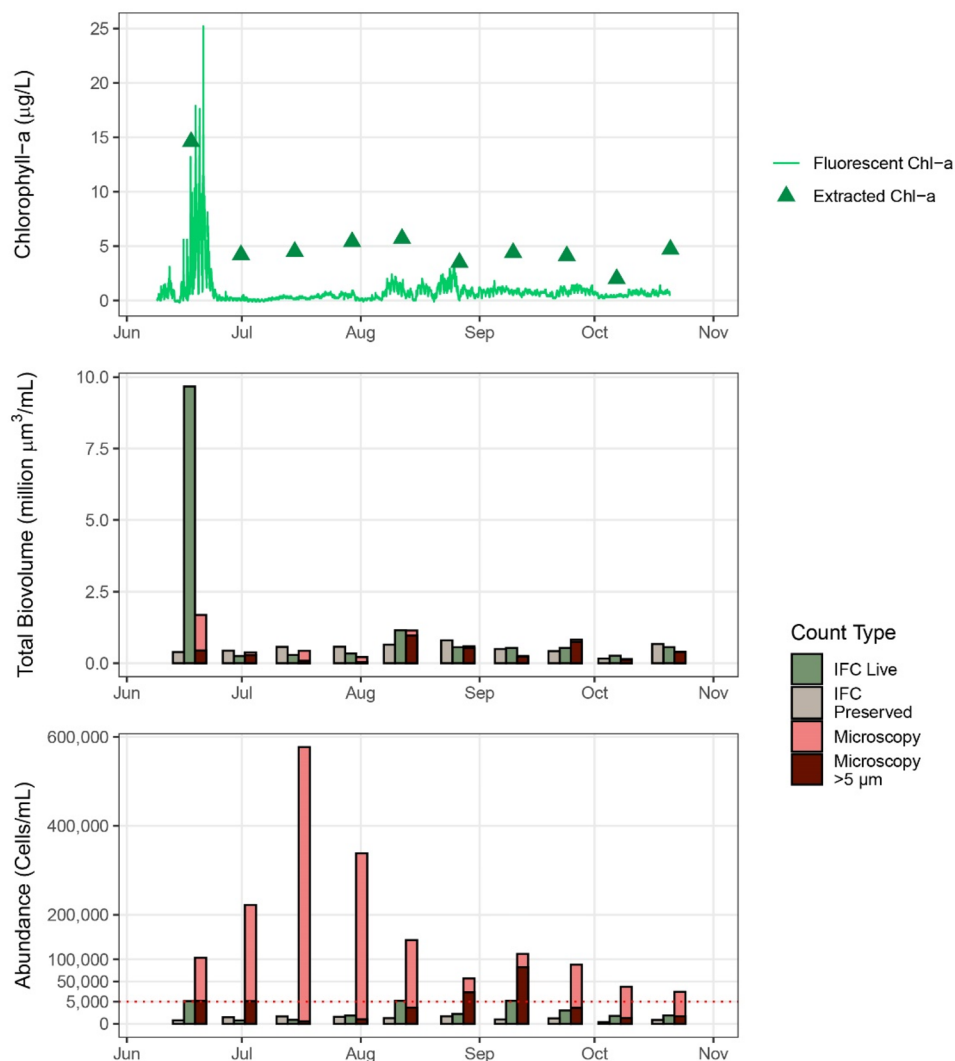


Figure 4. Multiple methods detected a *Uroglena* spp. bloom in Seneca Lake in Jun 2020. Sensor-based estimates of chlorophyll were measured continuously during Jun through Oct 2020 (green line, top panel) and discrete samples were measured for laboratory-extracted chlorophyll *a* (green triangles, top panel) and phytoplankton community biovolume (middle panel) and abundance (lower panel). Live and preserved phytoplankton samples were measured using imaging flow cytometry (IFC) and preserved samples were measured using microscopy. The scale below the red dotted line on the lower panel is a factor of 10 lower than the rest of the graph to allow for visualization of low abundances.

were observed in mid June; however, IFC preserved indicated a seasonal maximum in biovolume that occurred later in the season (Fig. 4). The live IFC biovolume estimate reflected the magnitude of the peak indicated by sensor- and laboratory-based measures of chlorophyll. In addition, the live IFC results indicated the bloom was caused by a chrysophyte, rather than HCB taxa. The peak indicated by sensor and laboratory-based measures of chlorophyll was not reflected in any of the abundance estimates. Interpretation of this event depends strongly on whether the sample was preserved or not, highlighting the importance of understanding how

preservation effects may influence phytoplankton identification and enumeration.

Microcystis aeruginosa bloom

In contrast to *Uroglena* spp., the IFC detected single cells from dissociated colonies of *Microcystis* spp. Owasco Lake experienced a substantial *M. aeruginosa* bloom during August 2020 (Fig. 2). Upon preservation, a much larger proportion of each sample was composed of single *M. aeruginosa* cells rather than intact colonies (Fig. 5). In live samples collected on August 12 and August 25, 74% and 66%, respectively, of the total cell

counts were comprised of cells within *M. aeruginosa* colonies. Upon preservation, 16% and 12%, respectively, of cells were within *M. aeruginosa* colonies. Similarly, the contribution of single cells to overall abundance increased from 2% to 80% in the August 12 sample and from 5% to 83% in the August 25 sample after preservation.

Relation between live and preserved imaging flow cytometry abundance and biovolume

In Owasco Lake, where the phytoplankton community was dominated by HCB taxa most of the season, live and preserved IFC estimates of abundance and biovolume were positively and significantly correlated (Table 2). Live IFC estimates of abundance were slightly lower than preserved estimates (Figs. 1 and 6). By comparison, live estimates of biovolume were substantially higher than preserved estimates (Fig. 6, Supplemental Fig. S2). Excluding the 2 August *M. aeruginosa* bloom samples from the analysis generally did not change or improve the overall relations, likely because *M. aeruginosa* was a predominant member of the phytoplankton community throughout the study period.

Relations between live and preserved IFC estimates of abundance and biovolume in Seneca Lake were not as straightforward (Fig. 6, Table 2). The relation between live and preserved biovolume estimates by IFC was positive; however, the relation between abundance estimates was negative. Neither correlation was statistically significant (Table 2). Live estimates of abundance tended to be higher than preserved estimates (Figs. 1 and 6), but the overall relation was strongly influenced by the 3 samples with the highest abundances (Fig. 6). Excluding the *Uroglena* spp. bloom sample, where known preservation effects were observed, did not improve the overall relation (Fig. 6, Table 2). In Owasco Lake, live estimates of biovolume were substantially higher than preserved estimates (Fig. 6, Supplemental Fig. S2). Unlike for abundance, excluding the *Uroglena* spp. bloom sample improved the overall relation between live and preserved estimates of biovolume, and the correlation between the 2 measures was statistically significant (Fig. 6, Table 2). Phytoplankton community composition was dynamic in both Seneca and Owasco lakes (Fig. 2), likely complicating the types of preservation effects that occurred and

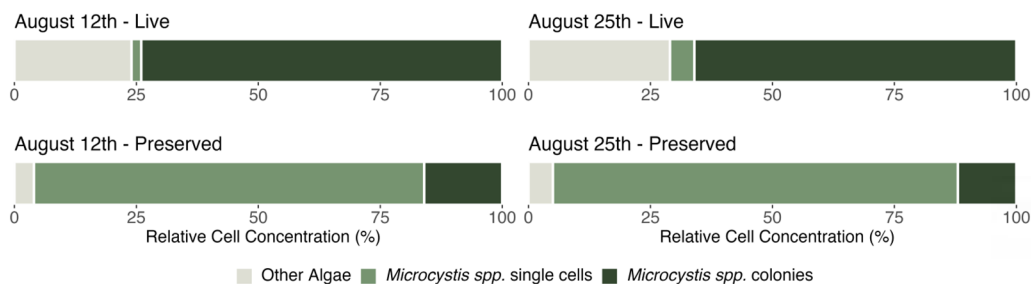


Figure 5. Relative contribution of unicellular and colonial *Microcystis* spp. to total phytoplankton abundance in live and preserved samples collected from Owasco Lake during a bloom in Aug 2020 and measured using imaging flow cytometry (IFC).

Table 2. Orthogonal regression and correlation coefficients for the relations between live and preserved estimates of abundance and biovolume measured by imaging flow cytometry.

	Regression (All data)		Regression (Bloom excluded)		Correlation (All data)		Correlation (Bloom excluded)	
	Slope	Intercept	Slope	Intercept	<i>r</i>	<i>P</i> value	<i>r</i>	<i>P</i> value
	Owasco Lake							
Biovolume	4.33	-3,500,224	1.65	-355,060	0.794	0.010*	0.595	0.132
Abundance	0.79	326	1.56	-928	0.927	<0.001*	0.881	0.007*
	Seneca Lake							
Biovolume	-76.76	41,201,376	2.35	-753,302	0.345	0.331	0.717	0.037*
Abundance	-17.69	24,375	-26.27	35,503	-0.248	0.492	-0.183	0.644

All $n=10$, except when bloom samples were excluded (Owasco: $n=8$; Seneca: $n=9$). Statistically significant correlations (P values < 0.05) are noted with an asterisk.

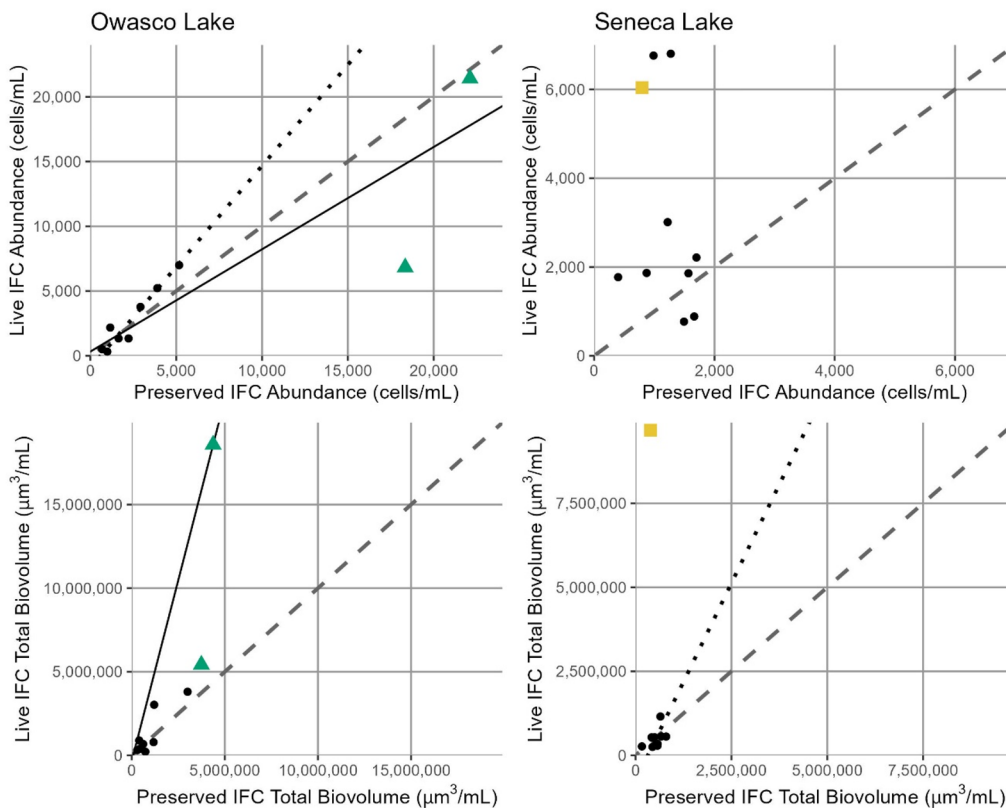


Figure 6. Relation between abundance (cells/mL) and biovolume ($\mu\text{m}^3/\text{mL}$) in live and preserved samples collected from Owasco and Seneca lakes during Jun through Oct 2020 and measured by imaging flow cytometry (IFC). Green triangles designate Aug 2020 *Microcystis* spp. bloom samples from Owasco Lake, and the yellow square designates a Jun 2020 *Uroglena* spp. bloom sample from Seneca Lake. The 1:1 line is dashed in all panels. Orthogonal regression lines with (solid lines) and without (dotted lines) bloom samples included show where relations were statistically significant.

the relations between the live and preserved measures of abundance and biovolume by IFC.

Discussion

Most studies that compare the use of IFC and microscopy abundance or biovolume estimates have focused on specific taxa or eliminated large portions of the assemblage by only analyzing a certain size fraction or functional group (Embleton et al. 2003, Campbell et al. 2013, Hrycik et al. 2019, Kraft et al. 2021). Here, we examined the entire phytoplankton community resolvable by each method and aggregated to the functional group level for ease of interpretation, with an emphasis on potential cyanotoxin-producing cyanobacteria (HCB). The use of IFC captured the dynamic community composition while detecting potential taxa of concern (both taste- and odor-causing and HCB organisms) at lower abundances than microscopy. Patterns in HCB abundance were similar between IFC and microscopy

estimates, with all methods showing the progression of a summer bloom in Owasco Lake and reflecting a lack of major HCB activity in Seneca Lake (Fig. 2). However, the rest of the community may not be as comparable, even at the functional group level (based on Bray–Curtis analysis). Interpretation of community level comparisons are dependent on the way that size thresholds for inclusion were characterized for this analysis. BG taxa with an average GALD of 7 or 8 μm , just above the $>5\mu\text{m}$ size threshold, dominated late in the season in the “Microscopy $>5\mu\text{m}$ ” category but were not captured by the preserved IFC (Fig. 2). Inherent differences in the methods also likely contributed to the overall comparability by Bray–Curtis; that is, microscopic counts do not categorize taxa into the miscellaneous or unknown functional groups. More rigorous analyses are needed to fully explore the similarities between taxa categorized in functional groups other than HCB.

The IFC method detected HCB taxa earlier in the season than microscopy, likely due to the larger sample volumes analyzed and the higher number of natural units cataloged by the instrument. In Owasco Lake, *Microcystis* was detected by IFC a month before it was detected in the counts (Table 1). These results indicate that IFC may have the potential for earlier detection of taxa of concern. The rapid turnaround time and low-level detection are important considerations when developing early warning systems for HCBs in freshwater ecosystems. Field-deployed IFC devices have already been used successfully in marine HAB early warning systems that target selected species (Campbell et al. 2013, Ruiz-Villarreal et al. 2022); our results demonstrate that IFC techniques developed for marine applications have the potential for use in freshwater environments.

Picoplankton and small nanoplankton with GALD < 5 µm are an important and often overlooked part of phytoplankton assemblages. Small plankton are often missed in microscopy approaches because of the use of plankton tows that by design only capture phytoplankton above a selected size threshold (Lehman et al. 2017, Hrycik et al. 2019), the use of microscopes that are not fluorescence enabled, or the use of chemicals for preservation that mask fluorescence. In this study, we used a fluorescence-enhanced HPMA counting methodology to broaden the size range of the plankton community that was captured compared to traditional microscopy to include nanoplankton and large picoplankton. The IFCB used in this study was not designed to measure plankton < 5 µm. As such, occurrence and abundance were not comparable to microscopy results (Figs. 1 and 2). Traditional flow cytometry approaches have been used to more fully characterize picoplankton communities in freshwaters (Crosbie et al. 2003). Field-deployable flow cytometry instruments can be configured to reliably detect picoplankton, but they have not been widely used in freshwater systems. While detection of picoplankton is possible with flow cytometry, the magnification and electronic thresholds required to do so result in the exclusion of larger taxa, including most colonial HCBs (Olson et al. 2003). Imaging and traditional flow

cytometry approaches may be used complementarily to fully characterize complete phytoplankton assemblages; however, additional research in freshwater systems is needed.

Preservation of samples affected IFC results, with changes in community composition that influenced the abundance and biovolume relations (Fig. 6). The dominant taxa in our study tended to be colonial, and dissociation effects were observed upon preservation. In addition, there was a strong preservation influence on biovolume for the taxa observed in our study. Biovolumes were significantly lower in preserved samples likely because of cell distortion, loss of sheaths, and other preservation effects (American Public Health Association 2022). Preservation changed the interpretation of community dynamics. For example, preserved IFC results did not reflect the bloom of *Uroglena* spp. in Seneca Lake due to colonial dissociation of this fragile chrysophyte taxon (Fig. 3). Preservation had less of an effect on abundance estimates of *Microcystis* spp., indicating that preservation may not limit the detection of these HCB taxa, likely due to the larger, more robust cells (Table 1). Relations in this analysis may have been affected by the relatively small number of samples and the predominant taxa in the lakes sampled. Additional studies focused on other taxa, including HCBs, will further our understanding of measurement error in IFC phytoplankton abundance and biovolume estimates. The differences in IFC-measured abundance and biovolume between live and preserved samples need to be taken into consideration when designing research and monitoring programs to ensure sampling objectives are met.

There is a substantial amount of error inherent to estimating biovolume, and results among analysts using the same method can be quite variable (Canfield et al. 2019). In our study, we essentially had 2 different analyses that used 2 different approaches to estimate phytoplankton abundance and biovolume. Microscopy and IFC abundance estimates were more similar than biovolume estimates. Biovolume estimates by IFC instrumentation do not readily distinguish between cells and their extracellular sheaths or mucilage. As such, IFC-based biovolume estimates are expected to be higher than microscopy estimates in assemblages dominated by

sheath/mucilage-bearing taxa. For example, the effectiveness of the biovolume estimation method of IFC instruments has been shown to be somewhat morphology specific. Hrycik et al. (2019) found that IFC analysis overestimated biovolume relative to microscopy, especially in coccoid cyanobacteria ($R^2 = 0.43$ for both methods of biovolume calculation), and generally showed a poor relationship for chrysophytes ($R^2 = 0.00$ and 0.01 for regressions of microscopy biovolume estimates and 2 methods of IFC biovolume calculations) but showed better regression relationships for the filamentous cyanobacteria group ($R^2 = 0.71$ and 0.73 for 2 methods of IFC biovolume calculation). By comparison, Kraft et al. (2021), found that IFC-based estimates of biovolume for 3 taxa of marine filamentous cyanobacteria correlated well with microscopy (*Aphanizomenon* $R^2 = 0.84$, *Dolichospermum* $R^2 = 0.82$, *Oscillatoriales* $R^2 = 0.56$). The dominant HCB taxa in our study was *Microcystis*, a coccoid cyanobacteria. As observed by Hrycik et al. (2019), both the live and preserved IFC estimates of HCB biovolume were significantly higher than estimates by microscopy in our study (and live estimates were significantly higher than preserved estimates). Higher biovolume estimates by IFC relative to microscopy may be caused by inclusion of the mucilage or overestimation of cell size (Graham et al. 2018, Hrycik et al. 2019).

Our study lakes had low non-algal turbidity and DOC, conditions that minimized the likelihood of matrix interferences with IFC use. Despite these ideal imaging conditions, we chose to manually assign images to taxonomic groups, rather than the more time-intensive reclassification of images using an IFC auto classifier. Hrycik et al. (2019) opted for a similar manual sorting approach in freshwater systems. Fully automated identification in the Baltic Sea demonstrated that IFC can be used to reliably track population dynamics of filamentous cyanobacteria in marine settings using an aut classifier (Kraft et al. 2021). More research would help to validate the automated classifier methodology in different types of freshwater systems, although other studies have shown that IFC methods have promise across a wider range of lake types than those included in our study (Graham et al. 2018, Hrycik et al. 2019).

There are IFC devices deployed in coastal monitoring networks on the east and west coasts of the United States (Anderson 2023, Woods Hole Oceanographic Institution 2023). These networks are focused on the identification and enumeration of marine HAB taxa with rigid structures, like diatom frustules and the theca of dinoflagellates, which are distinct and relatively large. Our study demonstrates that with the assistance of a trained algal taxonomist, IFC technology captures other functional groups and morphologies (e.g., chrysophytes and colonial coccoid cyanobacteria) that often dominate freshwater systems. The laboratory-based application of IFC in this study allowed receipt of results in 5 d or less, a substantial improvement over traditional microscopy, which can be time-consuming to conduct (Chorus and Welker 2021). Development of field-based IFC applications in freshwater has the potential to generate near-real-time information about phytoplankton community dynamics and the presence and abundance of potentially harmful taxa, comparable to existing marine networks (Anderson 2023, Woods Hole Oceanographic Institution 2023).

Overall, study findings indicate that laboratory-based use of IFC technology may be a valuable tool to detect and track HCB taxa in freshwater systems, but as for any tool there are strengths and limitations. Decisions between the analysis of live or preserved samples depend in large part on how quickly samples can be delivered to the laboratory. Live samples will avoid distortion and disruption of delicate cells caused by preservation, but in cases where overnight shipping of live samples is cost prohibitive or impractical, sample preservation becomes necessary. It is necessary to evaluate the data collection objective when deciding between methods. If a quick turnaround time is critical, laboratory-based IFC might be a better option, but if the goal is to understand the size structure of the phytoplankton community, including the picoplankton, epifluorescence microscopy or using a combination of microscopy and traditional flow cytometry may be preferable. Consistency in methodology over long-term projects is important and our results indicate caution is warranted when comparing metrics and applying thresholds based on one

methodology to results from another, particularly for biovolume estimates.

Acknowledgments

The authors dedicate this article to Dr. Ann St. Amand, whose vision, passion, and dedication to excellence in algal taxonomy were at the heart of this study. We thank the numerous USGS field personnel who helped collect data for this project and ultimately made this work possible, including Michael Stouder, Elizabeth Nystrom, Alexandra Adams, Matthew Jennings, and Karen Beaulieu. Special thanks to Rebecca Gorney for discussion and thoughtful reviews of the article.

Disclosure statement

Any use of trade, firm or product names is for descriptive purposes only and does not imply endorsement by the U.S. government. The authors declare no competing interests.

Funding

Funding to support this study was provided by the U.S. Geological Survey and the New York State Department of Environmental Conservation.

References

- American Public Health Association. 2022. Standard methods for the examination of water and wastewater. 23rd ed. Washington (DC): American Public Health Association.
- Anderson C. 2023. CA imaging FlowCytobot network. Southern California Coastal Ocean Observing System. <https://sccoos.org/ifcb/>.
- Berkman JAH, Canova MG. 2007. Algal biomass indicators. In U.S. Geological Survey techniques of water-resources investigations. Book 9, Chapter 7.4; p. 82. Reston (VA): U.S. Geological Survey. doi: [10.3133/twri09A7.4](https://doi.org/10.3133/twri09A7.4)
- Borchers HW. 2022. pracma: practical numerical math functions. R package version 2.3.8; [cited 24 Aug 2022]. Available from <https://CRAN.R-project.org/package=pracma>
- Campbell L, Henrichs DW, Olson RJ, Sosik HM. 2013. Continuous automated imaging-in-flow cytometry for detection and early warning of *Karenia brevis* blooms in the Gulf of Mexico. *Environ Sci Pollut Res Int.* 20(10):6896–6902. doi: [10.1007/s11356-012-1437-4](https://doi.org/10.1007/s11356-012-1437-4).
- Campbell L, Olson RJ, Sosik HM, Abraham A, Henrichs DW, Hyatt CJ, Buskey EJ. 2010. First harmful Dinophysis (dinophyceae, dinophysiales) bloom in the U.S. is revealed by automated imaging flow cytometry. *J Phycol.* 46(1):66–75. doi: [10.1111/j.1529-8817.2009.00791.x](https://doi.org/10.1111/j.1529-8817.2009.00791.x).
- Canfield DE, Bachmann RW, Hoyer MV, Johansson LS, Søndergaard M, Jeppesen E. 2019. To measure chlorophyll or phytoplankton biovolume: an aquatic conundrum with implications for the management of lakes. *Lake Reserv Manage.* 35(2):181–192. doi: [10.1080/10402381.2019.1607958](https://doi.org/10.1080/10402381.2019.1607958).
- Chorus I, Welker M, editors. 2021. Toxic cyanobacteria in water. 2nd ed. Boca Raton (FL): CRC Press on behalf of the World Health Organization, Geneva CH.
- Clarke KR, Gorley RN. 2015. PRIMER v7: user manual/tutorial. Plymouth (UK): PRIMER-E.
- Crosbie ND, Teubner K, Weisse T. 2003. Flow-cytometric mapping provides novel insights into the seasonal and vertical distributions of freshwater autotrophic picoplankton. *Aquat Microb Ecol.* 33:53–66. doi: [10.3354/ame033053](https://doi.org/10.3354/ame033053).
- Crumpton W G. 1987. A simple and reliable method for making permanent mounts of phytoplankton for light and fluorescence microscopy1. *Limnology & Oceanography.*32(5):1154–1159. doi: [10.4319/lo.1987.32.5.1154](https://doi.org/10.4319/lo.1987.32.5.1154).
- Dashkova V, Malashenkov D, Poulton N, Vorobjev I, Barteneva NS. 2017. Imaging flow cytometry for phytoplankton analysis. *Methods.* 112:188–200. doi: [10.1016/j.ymeth.2016.05.007](https://doi.org/10.1016/j.ymeth.2016.05.007).
- Edler L, Elbrächter M. 2010. The Utermöhl method for quantitative phytoplankton analysis. In: Karlson B, Cusack C, Bresnan E, editors. Microscopic and molecular methods for quantitative phytoplankton analysis. Paris (France): UNESCO: Intergovernmental Oceanographic Commission; p. 13–20.
- Embleton KV, Gibson CE, Heaney SI. 2003. Automated counting of phytoplankton by pattern recognition: a comparison with a manual counting method. *J Plank Res.* 25(6):669–681. doi: [10.1093/plankt/25.6.669](https://doi.org/10.1093/plankt/25.6.669).
- Foster GM, Graham JL, Bergamaschi BA, Carpenter KD, Downing BD, Pellerin BA, Rounds SA, Saraceno JF. 2022. Field techniques for the determination of algal pigment fluorescence in environmental waters: principles and guidelines for instrument and sensor selection, operation, quality assurance, and data reporting. In: U.S. Geological Survey techniques and methods. Book 1, Chap. D10; p. 34. Reston (VA): U.S. Geological Survey. doi: [10.3133/tm1D10](https://doi.org/10.3133/tm1D10).
- Gifford S, Stouder M, Beaulieu K. 2023. Imaging flow cytometry data for live and preserved phytoplankton samples from Owasco and Seneca Lakes, Finger Lakes Region, New York, 2020. U.S. Geological Survey data release. doi: [10.5066/P9D0QAB1](https://doi.org/10.5066/P9D0QAB1).
- Graham JL, Loftin KA, Ziegler AC, Meyer MT. 2008. Cyanobacteria in lakes and reservoirs—toxin and taste-and-odor sampling guidelines. In: U.S. Geological Survey techniques of water-resources investigations. Book 9, Chap A7.5; p. 61. Reston (VA): U.S. Geological Survey Publisher. doi: [10.3133/twri09A7.5](https://doi.org/10.3133/twri09A7.5).
- Graham MD, Cook J, Graydon J, Kinniburgh D, Nelson H, Pilienci S, Vinebrooke RD. 2018. High-resolution imaging particle analysis of freshwater cyanobacterial blooms. *Limnol Ocean Methods.* 16(10):669–679. doi: [10.1002/lom3.10274](https://doi.org/10.1002/lom3.10274).
- Harred LB, Campbell L. 2014. Predicting harmful algal blooms: a case study with *Dinophysis ovum* in the Gulf of Mexico. *J Plank Res.* 36(6):1434–1445. doi: [10.1093/plankt/fbu070](https://doi.org/10.1093/plankt/fbu070).
- Helsel DR, Hirsch RM, Ryberg KR, Archfield SA, Gilroy EJ. 2020. Statistical methods in water resources. In: U.S.

- Geological Survey techniques and methods. Book 4, Chap. A3; p. 458. Reston (VA): U.S. Geological Survey. doi: [10.3133/tm4A3](https://doi.org/10.3133/tm4A3).
- Hillebrand H, Dürselen C-D, Kirschtel D, Pollinger U, Zohary T. 1999. Biovolume calculation for pelagic and benthic microalgae. *J Phycol.* 35(2):403–424. doi: [10.1046/j.1529-8817.1999.3520403.x](https://doi.org/10.1046/j.1529-8817.1999.3520403.x).
- Hrycik AR, Shambaugh A, Stockwell JD. 2019. Comparison of FlowCAM and microscope biovolume measurements for a diverse freshwater phytoplankton community. *J Plank Res.* 41(6):849–864. doi: [10.1093/plankt/fbz056](https://doi.org/10.1093/plankt/fbz056).
- Interstate Technology and Regulatory Council. 2020. Strategies for preventing and managing harmful cyanobacterial blooms (HCB-1) Section 4. Monitoring. Washington (DC): Interstate Technology and Regulatory Council, HCB Team. <https://hcb-1.itrcweb.org/monitoring/>.
- Johnston BD, Graham JL, Foster GM, Downing BD. 2022. Technical note—performance evaluation of the PhytoFind, an in-place phytoplankton classification tool. U.S. Geological Survey Scientific Investigations Report 2022–5103; p. 36.
- Kraft K, Seppälä J, Hällfors H, Suikkanen S, Ylöstalo P, Anglès S, Kielosto S, Kuosa H, Laakso L, Honkanen M, et al. 2021. First application of IFCB high-frequency imaging-in-flow cytometry to investigate bloom-forming filamentous cyanobacteria in the Baltic Sea. *Front Mar Sci.* 8:1–17. doi: [10.3389/fmars.2021.594144](https://doi.org/10.3389/fmars.2021.594144).
- Lehman PW, Kurobe T, Lesmeister S, Baxa D, Tung A, Teh SJ. 2017. Impacts of the 2014 severe drought on the *Microcystis* bloom in San Francisco Estuary. *Harmful Algae.* 63:94–108. doi: [10.1016/j.hal.2017.01.011](https://doi.org/10.1016/j.hal.2017.01.011).
- McLane Research Laboratories Inc. 2020. IFCB Users Manual Rev 20.E.05. https://mclanelabs.com/wp-content/uploads/2020/05/McLane-IFCB-Manual.Rev_20.E.05.pdf.
- Ndlela LL, Oberholster PJ, Van Wyk JH, Cheng PH. 2016. An overview of cyanobacterial bloom occurrences and research in Africa over the last decade. *Harmful Algae.* 60:11–26. doi: [10.1016/j.hal.2016.10.001](https://doi.org/10.1016/j.hal.2016.10.001).
- New York State Department of Environmental Conservation, Clinkhammer A, Cook S, McCaffrey L, Prestigiaco AR, June S, Gorney R, Kishbaugh S, Mueller N. 2019. 2018 Finger Lakes water quality report. https://www.dec.ny.gov/docs/water_pdf/2018flwqreport.pdf.
- Olrik K, Blomqvist P, Brettum P, Cronberg G, Eloranta P. 1998. Methods for quantitative assessment of phytoplankton in freshwaters, part I. Stockholm (Sweden): Naturvårdsverket, Svensk miljöövervakning, Rapport 4860.
- Olson RJ, Shalapyonok A, Sosik HM. 2003. An automated submersible flow cytometer for analyzing pico- and nanophytoplankton: FlowCytobot. *Deep Sea Res Part I Oceanogr Res Pap.* 50(2):301–315. doi: [10.1016/S0967-0637\(03\)00003-7](https://doi.org/10.1016/S0967-0637(03)00003-7).
- Olson RJ, Sosik HM. 2007. A submersible imaging- in-flow instrument to analyze nano and microplankton: Imaging Flow Cytobot. *Limnol Oceanogr-Meth.* 5:195–203. doi: [10.4319/lom.2007.5.195](https://doi.org/10.4319/lom.2007.5.195)
- Ortiz J, Stackpoole S, Murphy JC. 2023. Compilation of state-level freshwater harmful algal bloom recreational and drinking water guidelines for the conterminous United States as of 2022. U.S. Geological Survey data release, doi: [10.5066/P9C84YAK](https://doi.org/10.5066/P9C84YAK).
- Paerl HW, Huisman J. 2009. Climate change: a catalyst for global expansion of harmful cyanobacterial blooms. *Environ Microbiol Rep.* 1(1):27–37. doi: [10.1111/j.1758-2229.2008.00004.x](https://doi.org/10.1111/j.1758-2229.2008.00004.x).
- Perkins SR, Stouder MDW, Beaulieu K. 2021. Phytoplankton data from Owasco, Seneca, and Skaneateles Lakes, Finger Lakes Region, New York, 2019–2020 (ver 2.1, June 2023). U.S. Geological Survey data release, doi: [10.5066/P9TP9T1D](https://doi.org/10.5066/P9TP9T1D).
- PhycoTech Inc. 2018. General Technical Approach. [cited 2024 Apr 1]. <https://www.phycotech.com/Portals/0/PDFs/GenTech.pdf>.
- Pick FR. 2016. Blooming algae: a Canadian perspective on the rise of toxic cyanobacteria. *Can J Fish Aquat Sci.* 73(7):1149–1158. doi: [10.1139/cjfas-2015-0470](https://doi.org/10.1139/cjfas-2015-0470).
- R Core Team. 2022. R: a language and environment for statistical computing. Vienna (Austria): R Foundation for Statistical Computing.
- Ruiz-Villarreal M, Sourisseau M, Anderson P, Cusack C, Neira P, Silke J, Rodriguez F, Ben-Gigirey B, Whyte C, Giraudeau-Potel S, et al. 2022. Novel methodologies for providing in situ data to HAB early warning systems in the European Atlantic Area: the PRIMROSE experience. *Front Mar Sci.* 9:1–23. doi: [10.3389/fmars.2022.791329](https://doi.org/10.3389/fmars.2022.791329).
- Spanbauer TL, Briseño-Avena C, Pitz KJ, Suter E. 2020. Salty sensors, fresh ideas: the use of molecular and imaging sensors in understanding plankton dynamics across marine and freshwater ecosystems. *Limnol Oceanogr Lett.* 5(2):169–184. doi: [10.1002/lol2.10128](https://doi.org/10.1002/lol2.10128).
- U.S. Geological Survey. variously dated. National field manual for the collection of water-quality data. U.S. Geological Survey Techniques of Water-Resources Investigations, book 9, chapters A1–A10. <https://water.usgs.gov/owq/FieldManual>.
- U.S. Geological Survey. 2016. National Water Information System data available on the World Wide Web (USGS Water Data for the Nation). [cited 2023 Sep 17]. doi: [10.5066/F7P55KJN](https://doi.org/10.5066/F7P55KJN).
- Vaughan L, Zamyadi A, Ajjampur S, Almutaram H, Freguia S. 2022. A review of microscopic cell imaging and neural network recognition for synergistic cyanobacteria identification and enumeration. *Anal Sci.* 38(2):261–279. doi: [10.1007/s44211-021-00013-2](https://doi.org/10.1007/s44211-021-00013-2).
- Wagner RJ, Boulger RW, Jr, Oblinger CJ, Smith BA. 2006. Guidelines and standard procedures for continuous water-quality monitors—Station operation, record computation, and data reporting (ver 1.0). In: U.S. Geological Survey techniques and methods. Book 1, chapter D3. Reston (VA): U.S. Geological Survey. doi: [10.3133/tm1D3](https://doi.org/10.3133/tm1D3).
- Woods Hole Oceanographic Institution. 2023. Northeast harmful algal blooms. HAB Observing Network – New England. <https://northeasthab.whoi.edu/bloom-monitoring/habon-ne>.
- Zarauz L, Irigoien X. 2008. Effects of Lugol's fixation on the size structure of natural nano-microplankton samples, analyzed by means of an automatic counting method. *J Plank Res.* 30(11):1297–1303. doi: [10.1093/plankt/fbn084](https://doi.org/10.1093/plankt/fbn084).